

# The complementary relationship in estimation of regional evapotranspiration: An enhanced Advection-Aridity model

Michael T. Hobbins and Jorge A. Ramírez

Department of Civil Engineering, Colorado State University, Fort Collins, Colorado

Thomas C. Brown

Rocky Mountain Research Station, U.S. Forest Service, Fort Collins, Colorado

**Abstract.** Long-term monthly evapotranspiration estimates from Brutsaert and Stricker's Advection-Aridity model were compared with independent estimates of evapotranspiration derived from long-term water balances for 139 undisturbed basins across the conterminous United States. On an average annual basis for the period 1962–1988 the original model, which uses a Penman wind function, underestimated evapotranspiration by 7.9% of precipitation compared with the water balance estimates. Model accuracy increased with basin humidity. An improved formulation of the model is presented in which the wind function and the Priestley-Taylor coefficient are modified. The wind function was reparameterized on a seasonal, regional basis to replicate independent proxy potential evapotranspiration surfaces. This led to significant differences from the original Penman wind function. The reparameterized wind function, together with a recalibrated Priestley-Taylor coefficient in the wet environment evapotranspiration formulation, reduced the underestimation of annual average evapotranspiration to only 1.15% of precipitation on an independent set of validation basins. The results offered here lend further support for Bouchet's hypothesis as it applies to large-scale, long-term evapotranspiration.

## 1. Introduction

Most potential evapotranspiration models calculate the drying power of the air as a function of the speed and the vapor pressure deficit of the advected air, but the models often differ in their formulations of the wind function, for which there is currently no standard parameterization [Brutsaert, 1982]. The two models examined by Hobbins *et al.* [this issue], Morton's [1983] Complementary Relationship Areal Evapotranspiration (CRAE) model and Brutsaert and Stricker's [1979] Advection-Aridity (AA) model, exhibit two very different approaches to parameterizing the effects of large-scale advection on regional evapotranspiration ( $ET_a$ ).

The CRAE model does not use observations of wind speed but, instead, calculates potential evapotranspiration using a vapor transfer coefficient  $f_T$  that is dependent on atmospheric pressure but not on wind speed. The AA model relies on the Penman wind function, which was formulated to reproduce point observations of evaporation [Penman, 1948]. Of all climatic inputs the AA model is most sensitive to observed wind speed, whereas the performance of the CRAE model is, to a large extent, independent of wind speed.

As demonstrated by Hobbins *et al.* [this issue], the AA model significantly underestimates  $ET_a$ , and its performance is highly dependent on basin climatology. To improve the AA model, it is necessary to examine its advection component: the wind function ( $f(U_r)$ ) in the potential evapotranspiration ( $ET_p^{AA}$ ) formulation and the Priestley-Taylor coefficient  $\alpha$  in the wet environment evapotranspiration ( $ET_w^{AA}$ ) formulation.

This paper reports on three methods to reformulate the AA

model: The first two attempt to detrend the performance of the model; the last one attempts to remove its bias. First, independent point observations of pan evaporation are used to recalibrate the wind function on a seasonal basis. Second, a proxy spatially distributed  $ET_p$  surface is used to recalibrate the wind function on a seasonal and regional basis. This proxy  $ET_p$  surface is generated by the CRAE model and is used to provide interpolated values for observed pan evaporation surfaces. Third, once the trend is removed, the Priestley-Taylor coefficient  $\alpha$  is optimized such that the errors incurred in closing the water balance have zero mean. The resulting improved AA model yields unbiased, near-zero mean (1.15% of annual precipitation) annual closure errors when validated against independent regional evapotranspiration estimates obtained from long-term, large-scale water balances for undisturbed basins in the conterminous United States.

## 2. Complementary Relationship

### 2.1. Hypothesis

The hypothesis of a complementary relationship [Bouchet, 1963] states that over areas of a regional scale and away from any sharp environmental discontinuities, there exists a complementary feedback mechanism between actual and potential evapotranspiration. Energy at the surface that, because of limited water availability, is not taken up in the process of actual evapotranspiration ( $ET_a$ ) increases the temperature and humidity gradients of the overpassing air and leads to an increase in  $ET_p$  equal in magnitude to the decrease in  $ET_a$ . This relationship is described by (1):

$$ET_a + ET_p = 2ET_w \quad (1)$$

Under conditions where  $ET_a$  equals  $ET_p$ , this rate is referred to as the wet environment evapotranspiration ( $ET_w$ ). Figure 1

Copyright 2001 by the American Geophysical Union.

Paper number 2000WR900359.  
0043-1397/01/2000WR900359\$09.00

of *Hobbins et al.* [this issue] illustrates the complementary relationship.

## 2.2. Advection-Aridity Model

In this section the components of the complementary relationship,  $ET_p$  and  $ET_w$ , are summarized for the AA model. For a more detailed treatment of this model, see *Hobbins et al.* [this issue] and *Brutsaert and Stricker* [1979]. In this model,  $ET_p^{AA}$  is calculated by combining information from the energy budget and water vapor transfer in the Penman equation, shown below in (2), and  $ET_w^{AA}$  is calculated based on derivations of the concept of equilibrium evapotranspiration under conditions of minimal advection, first proposed by *Priestley and Taylor* [1972], and shown in equation (7).  $ET_a$  is then calculated as a residual of (1).

The familiar expression for the Penman equation is

$$\lambda ET_p = \frac{\Delta}{\Delta + \gamma} Q_n + \lambda \frac{\gamma}{\Delta + \gamma} E_a, \quad (2)$$

where  $\lambda$  represents the latent heat of vaporization,  $\Delta$  is the slope of the saturated vapor pressure curve at air temperature,  $\gamma$  is the psychrometric constant, and  $Q_n$  is the net available energy at the surface. The second term of this combination approach represents the effects of large-scale advection in the mass transfer of water vapor and takes the form of a scaled factor of an aerodynamic vapor transfer term  $E_a$ .  $E_a$ , also known as the “drying power of the air,” is a product of the vapor pressure deficit ( $e_a^* - e_a$ ) and a “wind function” of the speed of the advected air  $f(U_r)$  of the form (3):

$$E_a = f(U_r)(e_a^* - e_a). \quad (3)$$

In (3),  $U_r$  represents the wind speed observed at  $r$  meters above the evaporating surface,  $e_a^*$  and  $e_a$  are the saturation vapor pressure and the actual vapor pressure of the air at  $r$  meters above the surface, respectively. The wind function  $f(U_r)$  is either theoretically or empirically derived. *Brutsaert and Stricker* [1979] suggested the following theoretical expression for the wind function under neutral, i.e., a stable atmospheric boundary layer, conditions:

$$f(U_r) = \frac{\varepsilon a_v k^2 U_r}{R_d T_a \ln[(z_2 - d_0)/z_{0v}] \ln[(z_r - d_0)/z_{0m}]} \quad (4)$$

In (4),  $\varepsilon$  is the ratio of the gas constant of dry air  $R_d$  to that of water vapor  $R_v$ ;  $a_v$  is the ratio of the eddy diffusivity to the eddy viscosity under neutral conditions;  $k$  is the von Karman constant;  $z_{0m}$  and  $z_{0v}$  are the roughness lengths for momentum and water vapor, respectively;  $T_a$  is the air temperature in kelvins;  $z_2$  is the height at which  $e_a$  is measured;  $d_0$  is the displacement height; and  $z_r$  is the height of the wind measurement.

However, in the context of modeling monthly regional  $ET_a$  with the complementary relationship the effects of atmospheric instability and the onerous data requirements rule out such theoretical formulations. *Penman* [1948] originally suggested the following empirical linear approximation for  $f(U_r)$ :

$$f(U_r) \approx f(U_2) = 0.0026(1 + 0.54U_2), \quad (5)$$

which, for wind speeds at 2-m elevation in  $\text{m s}^{-1}$  and vapor pressures in Pa, yields  $E_a$  in  $\text{mm d}^{-1}$ . This formulation of  $f(U_2)$  was first proposed [*Brutsaert and Stricker*, 1979] for use in the AA model operating at a temporal scale of a few days.

As demonstrated by *Hobbins et al.* [this issue, Figure 13], using this expression in the AA model yields estimates of  $ET_a^{AA}$  that increasingly underestimate  $ET_a$  with increasing mean annual wind speed, especially for wind speeds above  $4 \text{ m s}^{-1}$ . This demonstrates the sensitivity of the AA model to this expression of the wind function and highlights the need for a reparameterization of this component, which is then the focus of much of this paper.

While much work has been done in the agricultural arena to calibrate or reformulate the proposed wind function for use in the combination or Penman equation [e.g., *Allen*, 1986; *Van Bavel*, 1966; *Wright*, 1982], these formulations operate on a limited spatial and temporal scale, do not hypothesize feedbacks of a regional nature, and require local parameterizations of resistance and canopy roughness. Thus they are not applicable in predicting regional evapotranspiration.

Substituting (3) and the wind function (5) into the Penman equation (2) yields the expression for  $ET_p$  in (6) used by *Brutsaert and Stricker* [1979] in the original AA model:

$$\lambda ET_p^{AA} = \frac{\Delta}{\Delta + \gamma} Q_n + \lambda \frac{\gamma}{\Delta + \gamma} f(U_2)(e_a^* - e_a). \quad (6)$$

In formulating the AA model for use in 3-day time steps, *Brutsaert and Stricker* [1979] ignore any effect of atmospheric stability in the wind function term.

The AA model calculates  $ET_w$  [*Brutsaert and Stricker*, 1979] using the *Priestley and Taylor* [1972] partial equilibrium evaporation equation:

$$\lambda ET_w^{AA} = \alpha \frac{\Delta}{\Delta + \gamma} Q_n, \quad (7)$$

where  $\alpha = 1.28$ . A reexamination of the value of the Priestley-Taylor coefficient  $\alpha$  is provoked by results reported by *Hobbins et al.* [this issue], which indicate the opportunity to recalibrate this parameter to remove a consistent bias toward underestimation of  $ET_a^{AA}$ . Further support for such a reexamination is provided by work summarized by *Brutsaert* [1982]. An approximate value of  $\alpha = 1.26$  for water surfaces under conditions of minimal advection and in the absence of inversions and condensation from *Priestley and Taylor* [1972] is supported by other researchers: for well-watered grass ( $\alpha = 1.27 \pm 0.02$  for perennial ryegrass) [*Davies and Allen*, 1973] and for shallow lakes and ponds and saturated sedge meadow [*Stewart and Rouse*, 1976, 1977]. Reanalysis of *Priestley and Taylor's* [1972] results suggests  $\alpha = 1.28$ . Other, more significant variations are also reported, for example,  $\alpha = 1.05$  for short, well-watered Douglas fir [*McNaughton and Black*, 1973]. Work on a shallow lake [*DeBruin and Keijman*, 1979] found intradaily variations in  $\alpha$  ranging from 1.15 early in the day to 1.42 in the afternoon and seasonal variations ranging from 1.20 for August to 1.50 for April.

*Morton* [1983] suggests that  $\alpha = 1.32$  be used instead of  $\alpha = 1.26$  or 1.28, as the latter values were derived from averages across free water and land surfaces [*Priestley and Taylor*, 1972] and probably underestimate the value for land surfaces alone because of their greater roughness and heterogeneity. Recognizing the variability in estimates for this empirical parameter, its calibration is the focus of much of the work in this paper.

## 3. Methodology

### 3.1. Model Performance

All analyses were conducted at a 10-km cell size for the conterminous United States on a monthly basis for the water

year (WY) period 1962–1988. The data sets and equations used in the generation of estimates of evapotranspiration and the long-term, large-scale water balances are described in detail by *Hobbins et al.* [this issue]. Additional data sets, specifically those used in the two attempts at reparameterizing  $ET_p^{AA}$ , are described under the methodologies for which they were required.

In the manner of *Eagleson* [1978], and as described by *Hobbins et al.* [this issue], the long-term, steady state water balance is expressed as

$$ET_a^* = P - Y. \quad (8)$$

A single estimate of the long-term total evapotranspiration  $ET_a^*$  over the period WY 1962–1988 was calculated for each basin in the “complete set” of basins described by *Hobbins et al.* [this issue]. This set of 139 minimally impacted basins contains 351 eight-digit hydrologic unit codes (HUCs), constituting 17.4% of the conterminous United States, and is broken down according to basin size in Table 1 of *Hobbins et al.* [this issue].

The  $ET_a^*$  estimate, henceforth referred to as the “independent evapotranspiration estimate,” is compared with the long-term  $ET_a^{MODEL}$  estimate, summed from the monthly evapotranspiration estimates over the same period (WY 1962–1988), in a measure that provides a means to verify the models. This basin-specific measure of the performance of the model is called the “average annual water balance closure error” or “closure error.” As shown by *Hobbins et al.* [this issue], the closure error for each model  $\epsilon^{MODEL}$  is calculated for each basin, as a percentage of precipitation, from (9):

$$\epsilon^{MODEL} = \frac{\sum_{i=1}^{27} \sum_{j=1}^{12} (ET_{a(i,j)}^{MODEL} - ET_{a(i,j)}^*)}{\sum_{i=1}^{27} \sum_{j=1}^{12} P_{(i,j)}} 100\%, \quad (9)$$

where  $ET_a^{MODEL}$  is the model estimate of  $ET_a$  and  $i$  and  $j$  are the water year and month, respectively.

Nonzero closure errors must first be considered to be either an overprediction (positive closure error) or underprediction (negative closure error) of evapotranspiration by the model. Other possible explanations, not quantified in this study, are (1) violations of the assumptions inherent in (8), perhaps through the effects of groundwater pumping, surface water diversions, or violations of the assumption of negligible net groundwater flow out of the basin, all of which effects were presumably minimized by selecting the basins according to *Wallis et al.* [1991] and *Slack and Landwehr* [1992]; (2) violations of the assumption of stationarity in climatological forcing; (3) errors in the hydroclimatological record; and (4) errors induced by spatial interpolation of the climatic variables.

### 3.2. $ET_p$ Reparameterization

Combining (2) and (3) yields the following expression for back calculating the wind function  $f(U_2)$ :

$$f(U_2) = \left( ET_p^{INDEP} - \frac{\Delta Q_n}{\Delta + \gamma \lambda} \right) \frac{\Delta + \gamma}{\gamma(e_a^* - e_a)}. \quad (10)$$

In sections 3.2.1 and 3.2.2, methods for estimating a new regional, seasonal wind function are described. The first uses point observations of pan evaporation ( $ET_{pan}$ ) as an independent measure of potential evaporation  $ET_p^{INDEP}$ . The second

uses potential evapotranspiration surfaces generated by the CRAE model ( $ET_p^{CRAE}$ ) as a proxy for  $ET_p^{INDEP}$ . Both methods back calculate values for  $f(U_2)$ , which are regressed on observations of  $U_2$  to create the necessary  $U_2$ - $f(U_2)$  relationships. These regressed relationships are linear as the data do not support a more complex, nonlinear regression analysis. The AA model is then reformulated to reflect the new  $f(U_2)$  relationships, creating the AA(1) model from the  $ET_{pan}$  calibration and the AA(2) model from the  $ET_p^{CRAE}$  calibration.

**3.2.1. Estimates of  $ET_p^{INDEP}$  using  $ET_{pan}$  observations.** At a point in a homogeneous region of scale lengths of the order of 1–10 km, the complementary relationship indicates that a free water surface will evaporate at the potential rate  $ET_p$ . Thus, if the aerological conditions are known (i.e., temperature, humidity, and solar radiation), pan evaporation ( $ET_{pan}$ ) observations can be used on a seasonal (i.e., monthly) basis to back calculate the value of the drying power of the air  $E_a$ , and hence the value of the wind function  $f(U_2)$ , using (10), with  $ET_{pan}$  substituted for  $ET_p^{INDEP}$ . The values of  $f(U_2)$  are then combined with the observed wind speeds at the station to generate the empirical monthly relationships between  $U_2$  and  $f(U_2)$ , ( $U_2$ - $f(U_2)$ ).

Monthly pan evaporation ( $ET_{pan}$ ) data are drawn from the 14 stations across the conterminous United States in the National Climate Data Center (NCDC) data set (EarthInfo, NCDC Summary of the Day (TD-3200 computer file), Boulder, Colorado, 1998) that lay within 1 min of latitude and longitude of the Solar and Meteorological Surface Observation Network (SAMSON) stations [*National Oceanic and Atmospheric Administration*, 1993] from which the other climatological input data (average temperature, solar radiation, and humidity) are drawn. The geographic proximity threshold, although it limited the number of station observations, was chosen in order to ensure that the data from both of the two sources represented the same aerological conditions and therefore could be used in (10).

The resulting  $f(U_2)$  values are then compared, on a monthly basis, to the wind speeds observed at the SAMSON stations. For each month a least squares fit is derived to express this relationship. The AA model is reformulated to reflect the seasonal  $f(U_2)$  expressions, creating the AA(1) model, and the water balance closure errors ( $\epsilon^{AA(1)}$ ) are recalculated.

**3.2.2. Estimates of  $ET_p^{INDEP}$  using  $ET_p^{CRAE}$ .** The spatial patterns and values of the average annual  $ET_p^{CRAE}$  surface [*Hobbins et al.*, this issue, Figure 3a] closely match the contours of the climatological (1931–1960) surface of pan evaporation derived from spatially interpolated observations [*U.S. Geological Survey*, 1970]. Thus, in the absence of any other source of independent and spatially distributed  $ET_p$  data the monthly  $ET_p^{CRAE}$  surfaces are used as proxy  $ET_{pan}$  data. The Penman wind function in the AA model  $f(U_2)$  is then calibrated to the proxy  $ET_{pan}$  data.

The study area was divided into the 18 management regions defined by the U.S. Geological Survey (USGS) water resource regions (WRR). Two thirds of the original set of 139 basins were selected for a calibration subset, leaving the remaining one third for a validation subset. For the calibration subset, only basins containing a single HUC or a combination of two HUCs were selected, with each HUC appearing in one basin, at most. This resulted in a calibration subset of 92 basins containing 110 HUCs, covering an area of  $394 \times 10^3$  km<sup>2</sup>, or 4.9% of the conterminous United States.

Substituting spatially integrated  $ET_p^{CRAE}$  values for

$ET_p^{\text{INDEP}}$  in (10), and using monthly basin-wide depths for  $ET_p^{\text{CRAE}}$  and  $Q_n$  and monthly spatial averages for  $\Delta$ ,  $\gamma$ , and  $(e_a^* - e_a)$ , values of  $f(U_2)$  were back calculated for each month and each basin in the calibration subset in each WRR. Basin months for which constraints applied (i.e., months where  $\min(Q_n) < 0$ ,  $\min(e_a^* - e_a) < 0$ , or  $\min(ET_w) < 0$ ) were excluded. These values were then paired with the relevant monthly spatial averages of  $U_2$ , resulting in 26,040 paired values of  $f(U_2)$  and  $U_2$  spread between the 216 WRR-month combinations (i.e., 18 WRRs and 12 months).

In order to generate new regional, seasonal (monthly) wind functions, least squares linear regressions were conducted on the  $U_2$ - $f(U_2)$  relationship on a monthly and regional basis. Months that did not have sufficient data (i.e., fewer than an arbitrarily chosen 27 values) were infilled from surrounding months. One WRR (i.e., 16) did not have any data as there were no basins selected in this WRR. The regression for this WRR involved stations from surrounding WRRs (i.e., WRRs 10, 14, 15, 17, and 18) on the basis of their being the closest to the WRR in question.

Again, to test the performance of the new, regional, and seasonal wind function in the long-term, large-scale water balances, the AA model was reformulated to reflect these new regional, seasonal  $f(U_2)$ - $U_2$  relationships, creating the AA(2) model. The water balance closure errors ( $\varepsilon^{\text{AA}(2)}$ ) were recalculated for the full set of 139 basins following the procedures outlined in section 3.1.

### 3.3. $ET_w$ Recalibration

With  $ET_p^{\text{AA}}$  formulated to be independent of advection, attention must turn to removal of the negative bias in the AA(2) water balance closure errors. This bias results from the underestimation of  $ET_a$  and may be removed by increasing the Priestley-Taylor coefficient  $\alpha$  in (7). This would have the effect of increasing  $ET_w$  and hence  $ET_a$ .

For the calibration set of 92 basins previously described, monthly surfaces of  $ET_w$  were generated for a range of  $\alpha$  values in order to isolate the  $\alpha$  yielding a zero mean annual closure error  $\varepsilon^{\text{AA}}$ . Note that the regional, seasonal wind functions  $f(U_2)$  in the  $ET_p$  formulation described in section 3.2.2 were used in conjunction with each trial  $ET_w$  run. This recalibration results in the AA(2\*) model.

## 4. Results

Figures 1a and 1b summarize results from work reported by *Hobbins et al.* [this issue] on the original CRAE and AA models. Figure 1a presents the empirical distribution of the complete set of 139 closure errors for both models. Summary statistics are listed in Table 1. The ranges are approximately  $-25\%$  to  $+20\%$  for the CRAE model, with one high outlier above  $+30\%$ , and are  $-35\%$  to  $+15\%$  for the AA model, with five high outliers above  $30\%$ . Neither model yields closure errors that are normally distributed.

Figure 1b shows the relationship between  $\varepsilon^{\text{MODEL}}$  and mean annual basin wind speed. The CRAE results are included here to demonstrate the effects of its different advection formulation. The  $\varepsilon^{\text{AA}}$  are strongly negatively correlated with, and hence the AA model is very sensitive to, wind speed (slope of  $-0.1152$ ,  $R^2 = 0.36$ , and  $p < 0.05$ ). (A  $p$  value  $\leq 0.05$  indicates that the hypothesis of a slope significantly different from zero cannot be rejected at the 95% confidence level.) The  $\varepsilon^{\text{CRAE}}$  are weakly positively correlated with wind speed (slope

of 0.0238,  $R^2 = 0.04$ , and  $p < 0.05$ ). They are clustered around zero for the lowest wind speeds and increase in variability with increasing wind speed. This near independence of the CRAE model's performance with wind speed appears to support *Morton's* [1983] treatment of advection.

### 4.1. Reparameterization of $ET_p^{\text{AA}}$ Using $ET_{\text{pan}}$

Figure 2 shows an example (August) of the monthly  $f(U_2)$ - $U_2$  relationship derived by substituting point observations of  $ET_{\text{pan}}$  for  $ET_p^{\text{INDEP}}$  in (10). The least squares linear fit to the observed  $f(U_2)$ - $U_2$  relationship yields the following (11) for the August wind function in  $\text{mm month}^{-1}$ :

$$f(U_2) = 0.4703U_2 - 0.1954, \quad R^2 = 0.47, \quad p < 0.05. \quad (11)$$

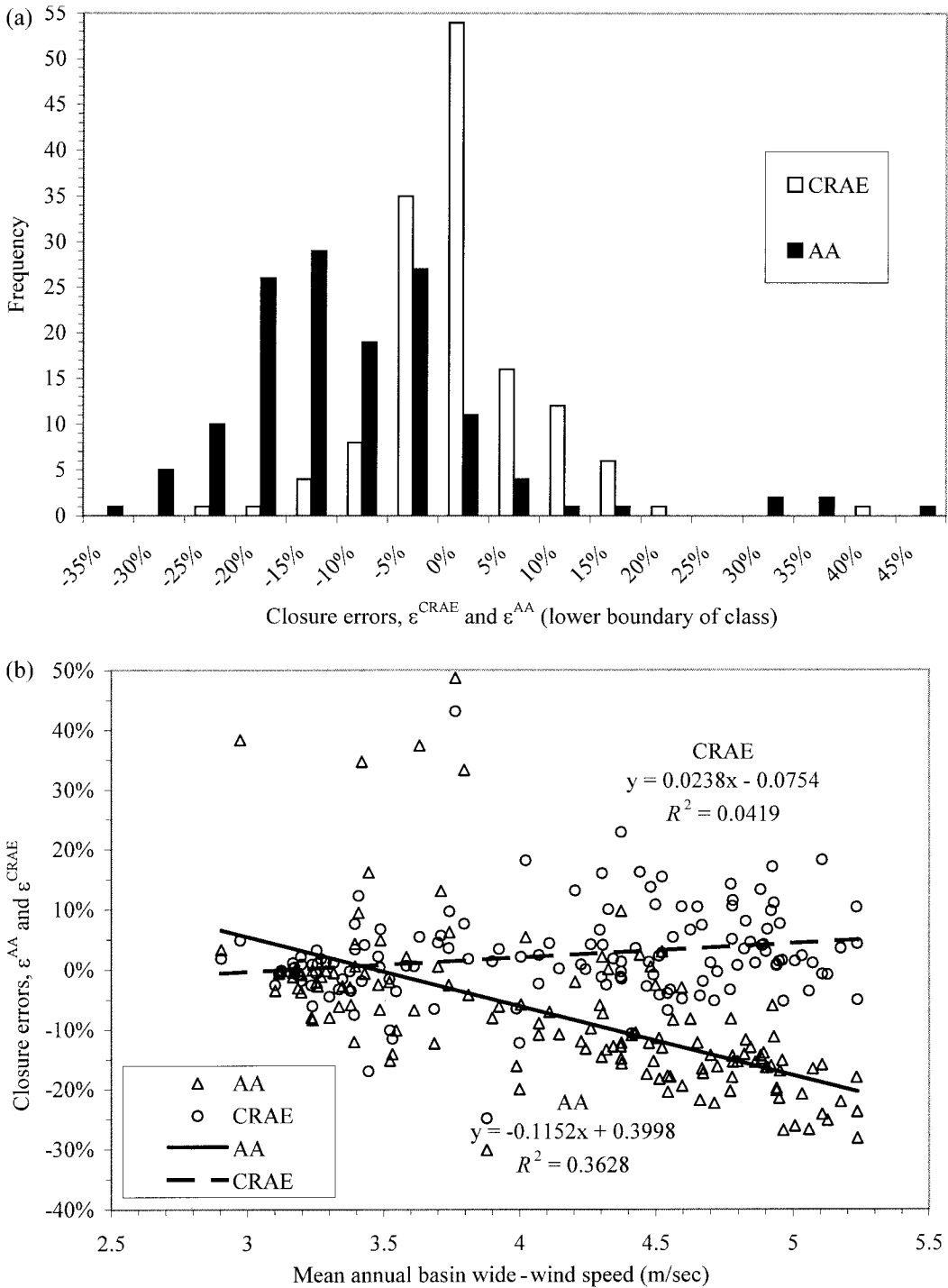
Graphically, the least squares linear fit for the observed  $f(U_2)$ - $U_2$  relationship, expressed in (11), is steeper and higher across the observed  $U_2$  range than that predicted by the Penman wind function, expressed in (5), used in the *Brutsaert and Stricker* [1979] AA model. The estimate for  $f(U_2)$  for August from (11) is then higher than that of the Penman wind function in (5), which, when compared to the AA model, leads to a higher estimate of  $ET_p$  and thereby a lower estimate of  $ET_a$ . This is, in fact, the case for all months in the growing season (May through September). For the rest of the year the magnitude of the observed  $f(U_2)$ - $U_2$  relationship is approximately equal to that of (5), although often slightly offset. Given that annual evapotranspiration totals are highly skewed toward warmer months, these differences should lead to increasingly negative water balance closure errors across the study basins when compared to the AA model.

Figure 3a indicates that this is, indeed, the case for the complete set of basins. The histogram of closure errors for the AA(1) model has shifted to the left, indicating that it is predicting a lower  $ET_a$  than the AA model. Although the skewness has decreased from 1.7501 for the  $\varepsilon^{\text{AA}}$  to  $-0.5117$  for the  $\varepsilon^{\text{AA}(1)}$ , reflecting a more normal distribution with a preponderance of negative values, the null hypothesis of normality must still be rejected. The mean closure error has decreased from  $-7.92\%$  to  $-27.05\%$ . The maximum and minimum also indicate this shift: from 48.71% to 16.47% and from  $-30.11\%$  to  $-74.21\%$ , respectively. The standard deviation also compares poorly: increasing from 12.67% to 18.98%.

Figure 3b shows the water balance closure errors  $\varepsilon^{\text{AA}(1)}$  plotted against mean annual wind speed. Included for comparison is the relationship already established [*Penman*, 1948; *Brutsaert and Stricker*, 1979] for the AA model. The most striking feature of this plot is that the closure errors for the AA(1) model show a stronger relationship to wind speed than do those of the AA model. Below about  $4 \text{ m s}^{-1}$ , the  $\varepsilon^{\text{AA}(1)}$  appear to be independent of wind speed. However, above  $4 \text{ m s}^{-1}$  the  $\varepsilon^{\text{AA}(1)}$  are strongly negatively correlated with wind speed. Thus, for a given wind speed the AA(1) model tends to overestimate  $ET_p$  and hence underestimate  $ET_a$  to an even greater degree than the original AA model. As this reformulation of the Penman wind function did not improve the performance of the AA model with respect to advection, no further work on it was performed.

### 4.2. Reparameterization of $ET_p^{\text{AA}}$ Using $ET_p^{\text{CRAE}}$

The general effects of the  $ET_p^{\text{CRAE}}$ -based reparameterization are illustrated in the results for WRR 11 (Arkansas-



**Figure 1.** (a) Histogram of closure errors  $\epsilon^{CRAE}$  and  $\epsilon^{AA}$ . (b) Closure errors  $\epsilon^{CRAE}$  and  $\epsilon^{AA}$  versus mean annual basin-wide wind speed.

White-Red region). Figure 4a shows the monthly  $f(U_2)-U_2$  relationships derived by substituting for  $ET_p^{INDEP}$  in (10) the 1150 monthly basin-wide totals of  $ET_p^{CRAE}$  from the five calibration basins in WRR 11. In Figures 4a the solid lines represent the least squares linear fit of these relationships; the dashed lines represent the original, nonseasonal Penman wind function used in the *Brutsaert and Stricker* [1979] AA model, expressed mathematically in (5). There are two prominent findings from these plots.

First, for all months the slope of the relationship between  $U_2$

and  $f(U_2)$  is less than that predicted by the Penman wind function in (5). This indicates that the effects of increasing wind speeds on the value of  $ET_p$  are less pronounced than for the Penman wind function used in the AA model. From March to September the relationship between  $U_2$  and  $f(U_2)$  is still positive in common with empirical wind functions in general. From October to February, however, the relationship is negative. Within these months, applying the derived regional, seasonal wind functions would lead to lower estimates of  $ET_p$  for higher values of  $U_2$  and vice versa. This is contrary to the

**Table 1.** Summary Statistics for Water Balance Closure Errors

Model	Percent Mean Annual Basin-Wide Precipitation					
	Mean	Median	Minimum	Maximum	Standard Deviation	Skewness
CRAE (complete)	2.35	1.24	-24.87	43.13	7.69	0.9908
AA validation <sup>a</sup>	-8.56	-12.23	-26.69	38.31	13.45	1.6751
AA complete	-7.92	-10.55	-30.11	48.71	12.67	1.7501
AA(1) complete	-27.05	-24.36	-74.21	16.47	18.98	-0.5117
AA(2) calibration	-6.17	-6.91	-30.99	-7.79	9.25	1.1917
AA(2) validation	-7.93	-8.21	-17.75	7.10	5.32	1.0156
AA(2) complete	-6.76	-7.38	-30.99	37.79	8.16	1.3547
AA(2*) calibration	0.00	-2.02	-25.35	49.55	10.51	1.5358
AA(2*) validation	-1.15	-1.65	-12.16	19.59	6.66	1.0886
AA(2*) complete	-0.39	-1.80	-25.35	49.55	9.37	1.6049

<sup>a</sup>Refers to those sets of basins used to validate the AA(2) and AA(2\*) models.

Penman wind function (5), which predicts increasing  $f(U_2)$ , and hence increasing  $ET_p^{AA}$ , for increasing  $U_2$ .

In general, of the total of 197 directly observed (i.e., not filled in from surrounding data)  $f(U_2)$ - $U_2$  relationships derived for all months and regions, only one has a slope more positive than the Penman wind function (5). In fact, 110 of the slopes of observed  $f(U_2)$ - $U_2$  relationships are negative.

Second, the data for November through June lie predominantly below the line predicted by the Penman wind function (5), leading to lower estimates of  $ET_p^{AA}$  than those predicted by the Penman wind function. This, in turn, would lead to increasing estimates of  $ET_a^{AA}$ . The data for the other months, July through September, lie approximately on the Penman line. Thus, for a given wind speed during these summer months the AA(2) model would predict similar values to those of the AA model, dependent on the wind speed. Given that slopes of the  $f(U_2)$ - $U_2$  relationships in these months are lower than the Penman, one would expect, when compared to the AA model, to see higher estimates of  $ET_p$  for lower wind speeds and vice

versa. It should be noted, however, that the months with the positive slopes, as predicted by other empirical  $f(U_2)$  formulations, are those months with the highest  $R^2$  values for the regressed relationship (between 0.39 and 0.65).

Evapotranspiration totals in the annual cycle are highly skewed toward warmer months (July through October), for which the  $f(U_2)$ - $U_2$  relationships established using the AA(2) model are similar to, but at a lower slope than, the Penman wind function in (5). The combined effects of these differences and those of the remaining months (November through June), for which the derived relationships are both lower and at a lower slope than the Penman wind function in (5), upon the long-term, large-scale water balances would be difficult to predict. The mean monthly values of wind speed for the basins in WRR 11 are the lowest for the warmest months and, in fact, lie in the regions of the relationships established for these months that are to the left of the Penman line. Hence, in general, higher  $ET_p$  estimates and correspondingly lower  $ET_a$  estimates should be expected for these months. Three of the five closure

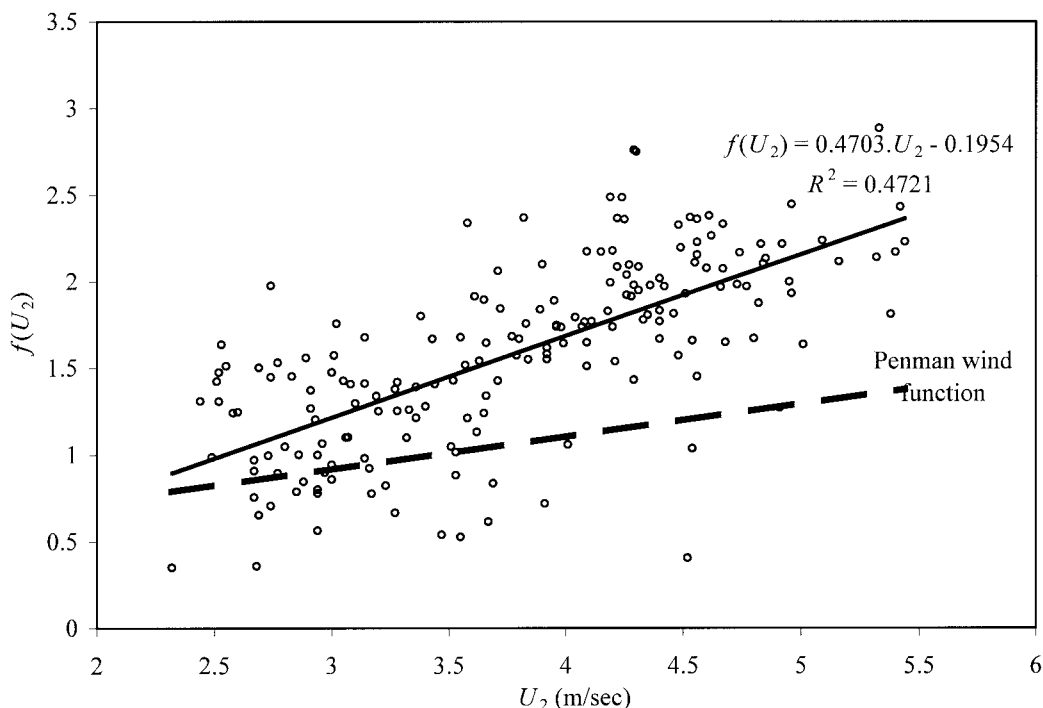


**Figure 2.** Example monthly  $f(U_2)$ - $U_2$  relationship for August.

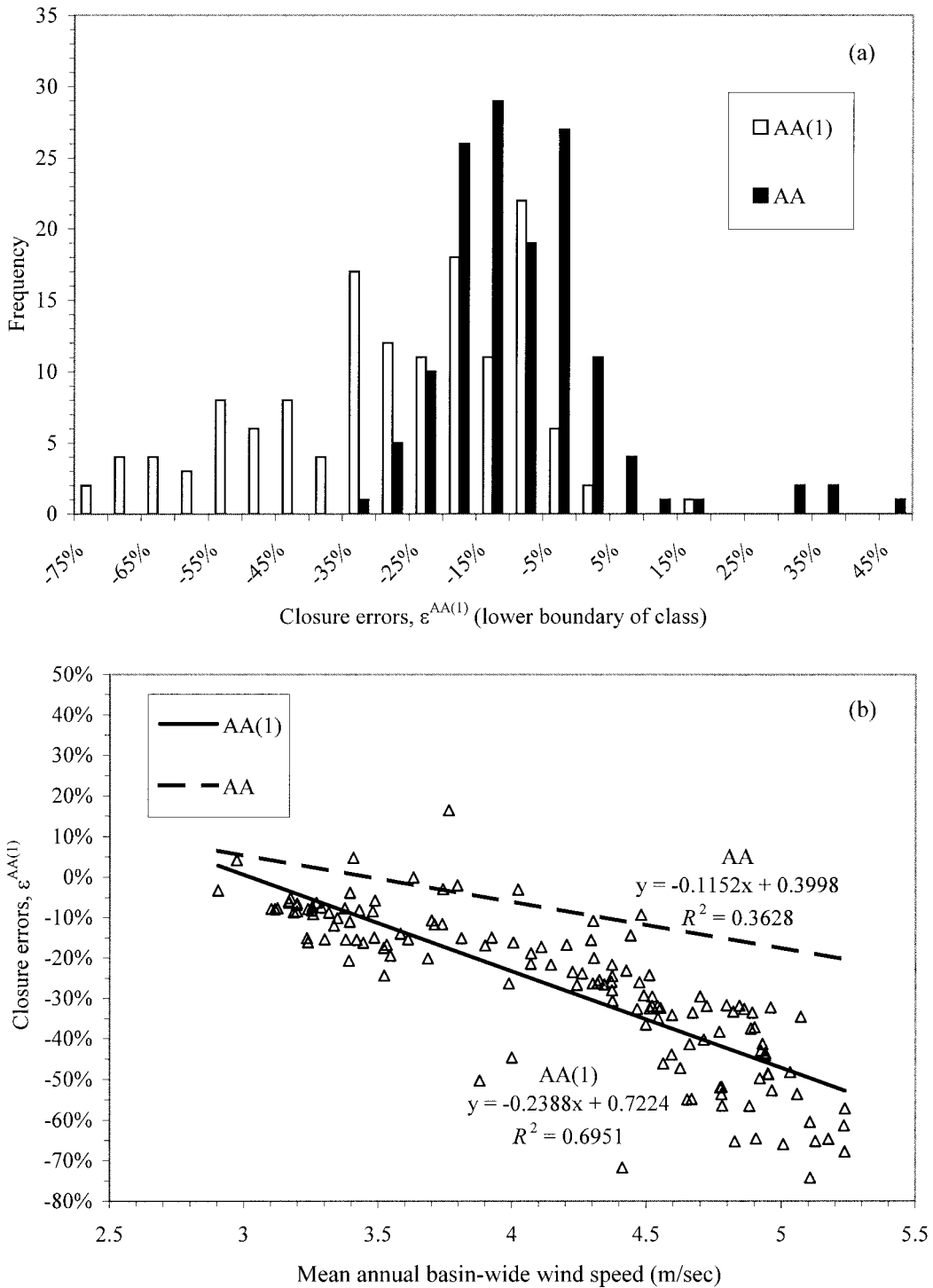


**Figure 3.** (a) Histogram of closure errors  $\epsilon^{AA}$  and  $\epsilon^{AA(1)}$ . (b) Closure errors  $\epsilon^{AA(1)}$  versus mean annual basin-wide wind speed.

errors of the calibration basins in WRR 11 decrease from the AA model to the AA(2) model (from  $-4.25\%$  to  $-5.83\%$ , from  $-5.84\%$  to  $-6.52\%$ , and from  $-10.88\%$  to  $-11.20\%$ ). The other two increase (from  $-18.00\%$  to  $-0.71\%$  and from  $-28.16\%$  to  $-18.43\%$ ). Of the two validation basins in WRR 11, one closure error increases (from  $-23.73\%$  to  $-7.38\%$ ), while the other decreases (from  $-2.60\%$  to  $-3.66\%$ ). The fact that the effect of this reparameterization on the closure errors for the basins in WRR 11 is so mixed indicates that, to varying

degrees, the underestimation in  $ET_a$  engendered in the calmer summer months is mitigated by the overestimation in the other windier months.

In general, the combination of the changes in  $ET_p^{AA}$  (i.e., the lower slopes and values of the observed relationships when compared with the Penman wind function (5)) wrought by the regional, seasonal  $f(U_2)-U_2$  relationships should therefore be to decrease the monthly  $ET_a^{AA}$  estimates for basin months with high wind speeds, while, especially from November to June,

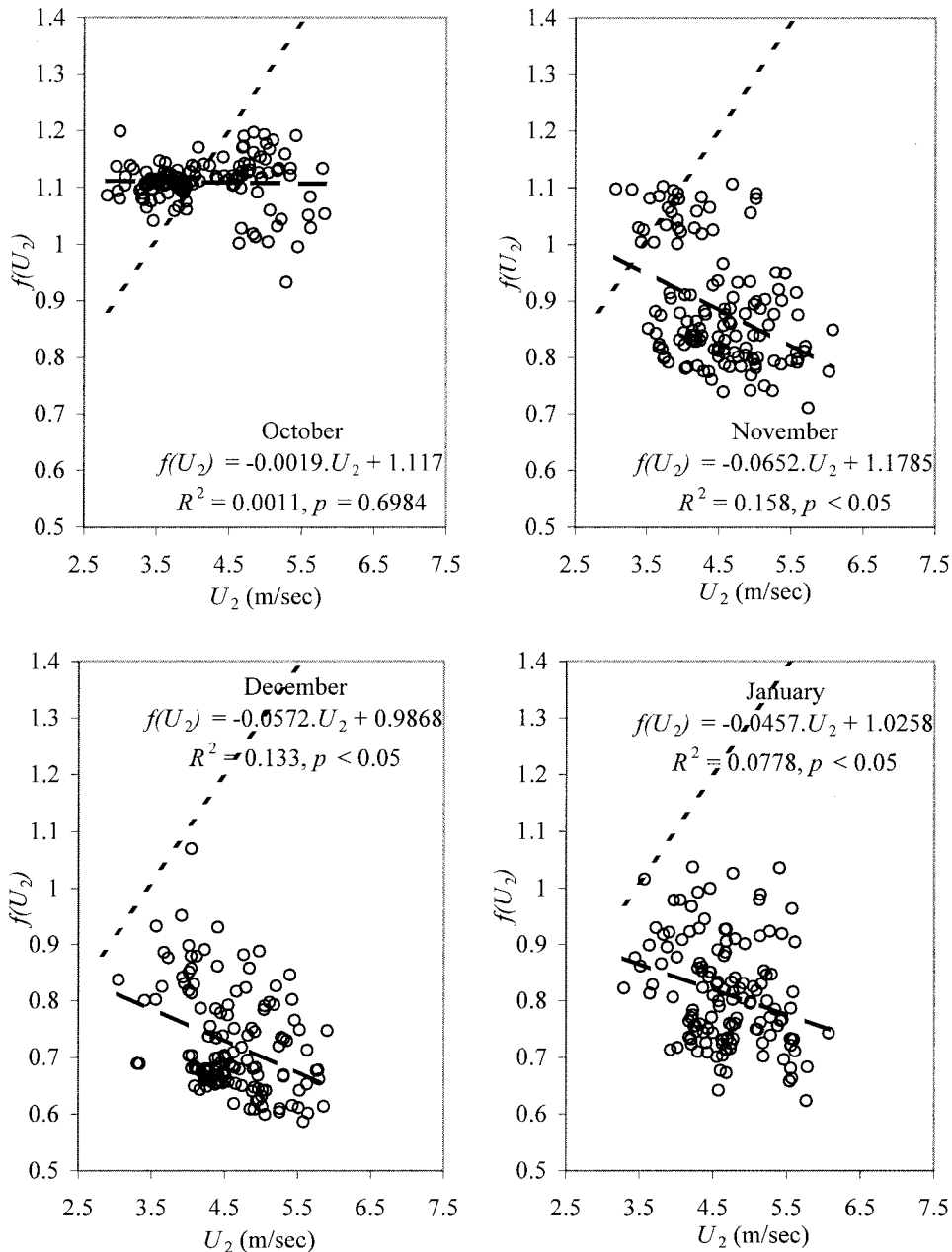


**Figure 4a.** Example of regional, seasonal  $f(U_2)$ - $U_2$  relationships: region 11 for October, November, December, and January; February, March, April, and May; and June, July, August, and September.

having little effect on basin months with lower wind speeds. This should have the effect of reducing the apparent dependence of the closure errors upon wind speed observed in Figure 1b.

Figure 4b displays the empirical frequency distributions of closure errors for the validation and combined (complete) basin sets in the AA(2) model and the original AA model. For the validation basin set the distribution of  $\varepsilon^{\text{AA}(2)}$  appears to be more normal than that of  $\varepsilon^{\text{AA}}$ , as reflected in the reduction of the skewness from 1.6571 for  $\varepsilon^{\text{AA}}$  to 1.0156 for  $\varepsilon^{\text{AA}(2)}$ . However, the null hypothesis of normality must still be rejected at the 95% significance level. For the validation set of basins the mean has increased from  $-8.56\%$  for  $\varepsilon^{\text{AA}}$  to  $-7.93\%$  for  $\varepsilon^{\text{AA}(2)}$ , and the standard deviation has decreased from  $13.45\%$  for  $\varepsilon^{\text{AA}}$  to  $5.32\%$  for  $\varepsilon^{\text{AA}(2)}$ . In applying the AA(2) model, of the five outliers, defined as  $\varepsilon^{\text{MODEL}}$  values above  $+30\%$ , four

have significantly improved  $\text{ET}_a$  estimates (closure errors have gone from  $+38.31\%$  to  $+7.10\%$ , from  $+33.34\%$  to  $+16.59\%$ , from  $+37.42\%$  to  $+14.45\%$ , and from  $+34.69\%$  to  $-6.58\%$ ), while the fifth has improved from  $\varepsilon^{\text{AA}} = +48.71$  to  $\varepsilon^{\text{AA}(2)} = +37.79\%$ . These outliers are discussed at some length by *Hobbins et al.* [this issue]. Summary statistics for both models are presented in Table 1.

Figure 4c shows the  $\varepsilon^{\text{AA}(2)}$  sets plotted against mean annual basin-wide wind speed. The relationship of  $\varepsilon^{\text{AA}(2)}$  with respect to wind speed derived as a result of this parameterization appears to be independent of mean annual wind speed. As regards the validation basin set, the least squares linear fit is nearly horizontal (slope of  $-0.0275$ ,  $R^2 = 0.14$ , and  $p < 0.05$ ). Included for comparison in Figure 4c is the linear relationship established for the original AA model.

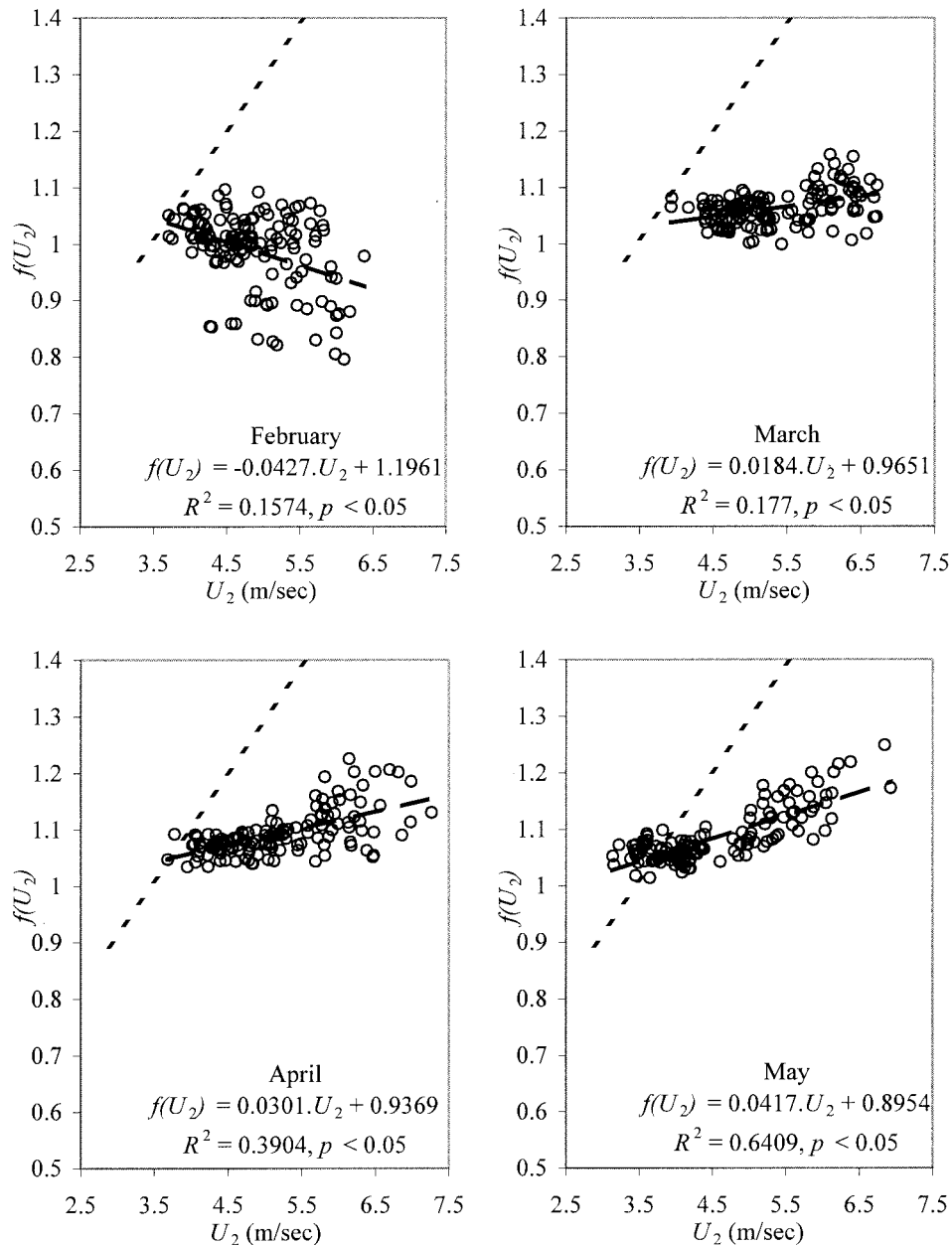


Figure 4a. (continued)

Although the relation of wind speed to closure error appears to have been removed in the AA(2) model, the consistent underestimation may be best addressed by recalibrating a component of the complementary relationship that is independent of wind speed, namely, the  $ET_w^{AA}$  component.

4.3.  $ET_w$  Recalibration

Figure 5 shows the AA(2) mean closure errors of the calibration set for each trial value of  $\alpha$ . The relationship between water balance closure error and  $\alpha$  yields a zero mean closure error at  $\alpha = 1.3177$ . Although equations (1), (7), and (9) suggest that this relationship should be approximately linear, that the relationship is so linear is surprising given the constraints on the values of the components of the complementary relationship, all of which have the effect of rendering this relationship nonlinear. Note that the standard deviation of the

calibration set of closure errors increases with increasing  $\alpha$  and moves from  $\sigma(\epsilon^{AA}) = 9.25\%$  for the original value of  $\alpha = 1.28$  to  $\sigma(\epsilon^{AA}) = 10.51\%$  for the recalibrated value of  $\alpha = 1.3177$ .

Figure 6a shows a histogram of the complete set of AA(2\*) closure errors resulting from using the value of  $\alpha$  of 1.3177 (i.e., the value that minimizes the mean closure error) in conjunction with the seasonally, regionally reparameterized wind function. Also shown in Figure 6a are the histograms for the complete runs of the AA and AA(2) models. Table 1 includes the summary statistics for the AA(2\*) model for the validation and calibration runs and for the complete set of basins.

In adapting the AA(2) model to the AA(2\*) model, which uses the optimized value of  $\alpha = 1.3177$  in its  $ET_w$  formulation, the main effect has been to shift the distribution to the right. This leads to an improvement in model performance, which is reflected in the summary statistics for the validation sets of both

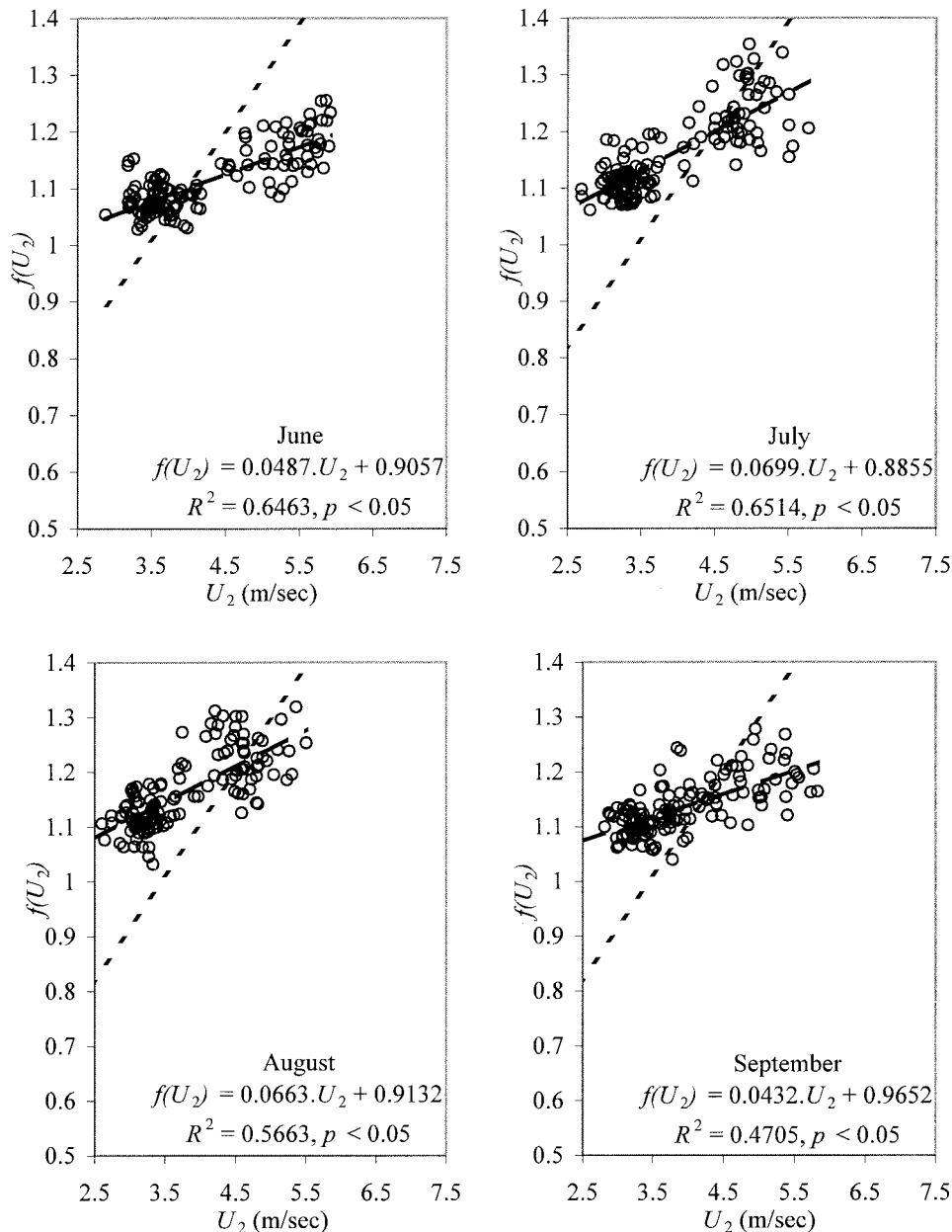


Figure 4a. (continued)

the AA(2) and the AA(2\*) runs. In progressing from the AA(2) model to the AA(2\*) model, the median closure error of the validation set has increased from  $-8.21\%$  to  $-1.65\%$ , and the mean has increased from  $-7.93\%$  to  $-1.15\%$ . The standard deviation for the validation set has increased from  $5.32\%$  to  $6.66\%$ , but there is little change in the skewness, from  $1.0156$  to  $1.0886$ , with the null hypothesis of normality rejected for both validation sets. For the complete set of basins the AA(2\*) model (skewness of  $1.6049$ ) still represents an improvement over the original AA model (skewness of  $1.7501$ ) as far as normality is concerned.

Figures 6b through 6d display the effects of basin climatology on the performance of the AA(2\*) model. Included on Figures 6b–6d are the least squares linear fits to the  $\varepsilon^{\text{AA}(2^*)}$  results for the validation, calibration, and complete basin sets. Also shown are the linear fits for the complete set of closure errors  $\varepsilon^{\text{AA}}$  for the original AA model. The  $\varepsilon^{\text{AA}}$  data themselves are displayed by *Hobbins et al.* [this issue] in Figures 11a

(precipitation), 11b ( $\text{ET}_a^*$ ), and 13 (wind speed). The regression analyses described below refer to the complete basin set.

As expected, the results for wind speed (Figure 6b) indicate a significant improvement over the original AA model (slope of  $-0.1152$ ,  $R^2 = 0.36$ , and  $p < 0.05$ ). The least squares linear fit lies almost directly along a line described by  $\varepsilon^{\text{AA}(2^*)} = 0$  (slope of  $-9.73 \times 10^{-4}$ ,  $R^2 = 5 \times 10^{-5}$ , and  $p = 0.09359$ ), indicating that the wind speed dependence evident in the original AA model has been eliminated. Also, the negative bias (i.e., toward underestimation of  $\text{ET}_a$ ) evident in the results for the original AA model and the AA(2) model (see Figure 4c) has been completely removed.

Regression analysis on the precipitation data (Figure 6c) indicates that, although there is no significant relationship (slope of  $4 \times 10^{-5}$ ,  $R^2 = 0.01$ , and  $p = 0.22$ ) between precipitation and  $\varepsilon^{\text{AA}}$ , the  $\varepsilon^{\text{AA}(2^*)}$  decrease very slightly (slope

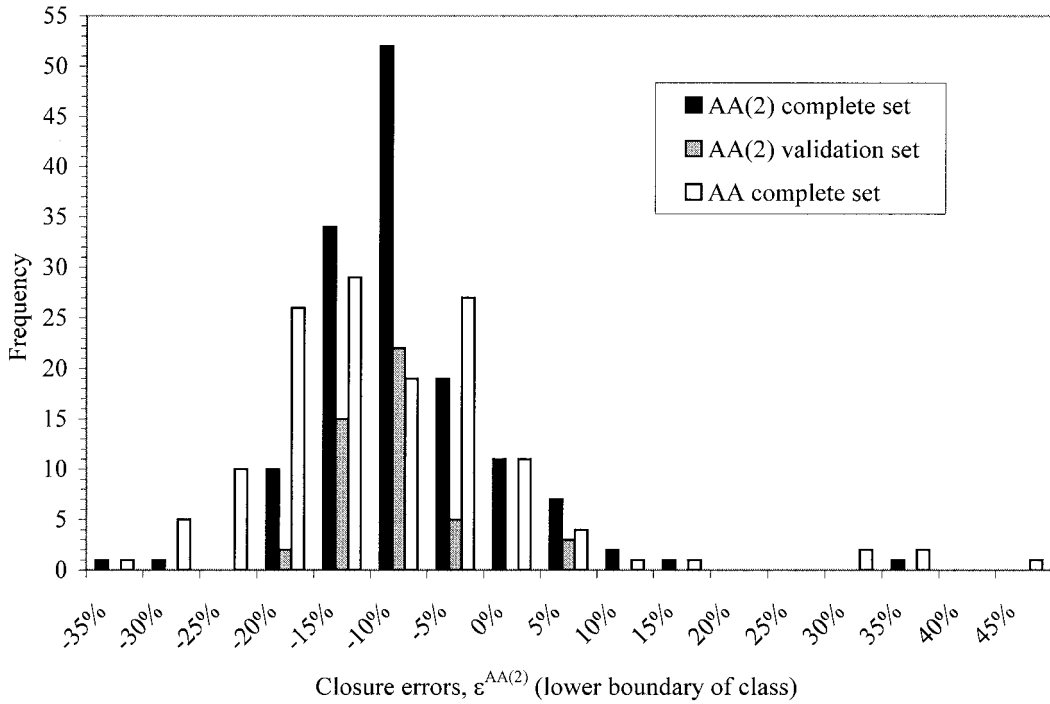


Figure 4b. Histogram of closure errors  $\epsilon^{AA(2)}$ .

of  $-8.5 \times 10^{-5}$ ,  $R^2 = 0.11$ , and  $p < 0.05$ ) with precipitation. The  $R^2$  value indicates that the  $\epsilon^{AA(2^*)}$  stick close to this relationship; also there is no bias, as previously discussed. The AA(2\*) model tends to overestimate  $ET_a^*$  for basins with less than  $700 \text{ mm yr}^{-1}$  of precipitation and underestimate for basins over  $700 \text{ mm yr}^{-1}$ . A basin at  $3100 \text{ mm yr}^{-1}$  is not shown, although it is included in the analysis of the calibration and complete sets.

Although the slope of the relationship between  $ET_a^*$  and

$\epsilon^{AA(2^*)}$  (Figure 6d) indicates a somewhat stronger negative relationship (slope of  $-2.2 \times 10^{-4}$ ,  $R^2 = 0.14$ , and  $p < 0.05$ ) than between  $ET_a^*$  and  $\epsilon^{AA}$ , the  $R^2$  value indicates that the  $\epsilon^{AA(2^*)}$  adhere to the regressed relationship more closely than in the case of the AA model (slope of  $-5.4 \times 10^{-5}$ ,  $R^2 = 4.4 \times 10^{-3}$ , and  $p = 0.44$ ). Also, the slope of the regressed relationship for the  $\epsilon^{AA}$ , although nominally flatter, is not statistically significant at the 95% level. This is borne out by examining Figure 11b of *Hobbins et al.* [this issue].

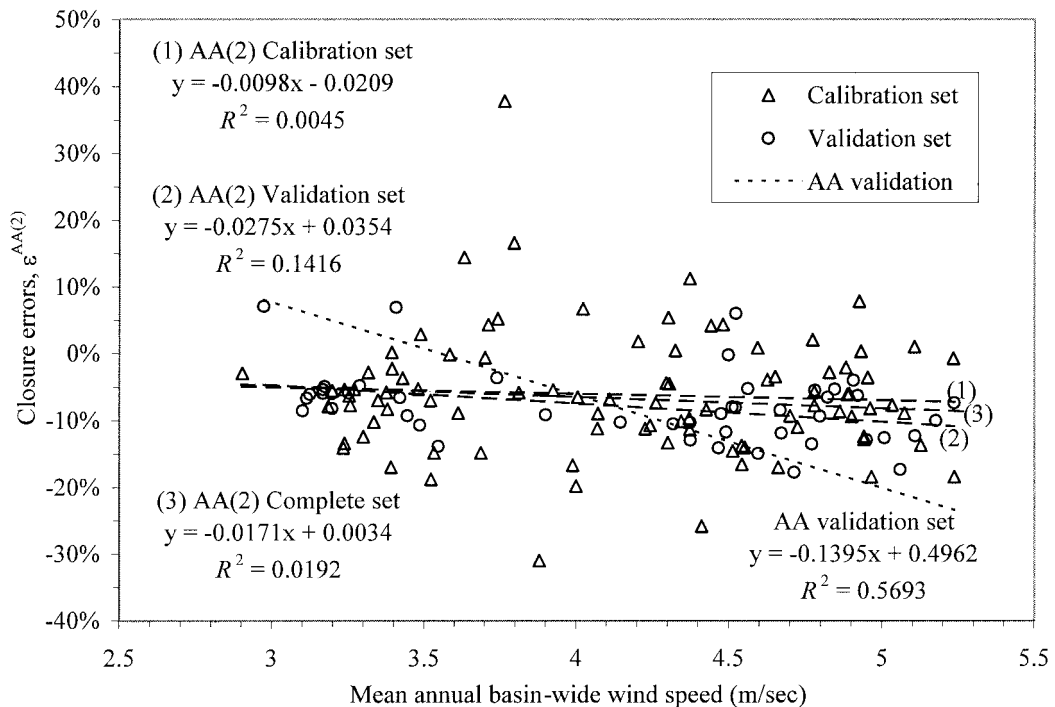


Figure 4c. Closure errors  $\epsilon^{AA(2)}$  versus mean annual basin-wide wind speed.

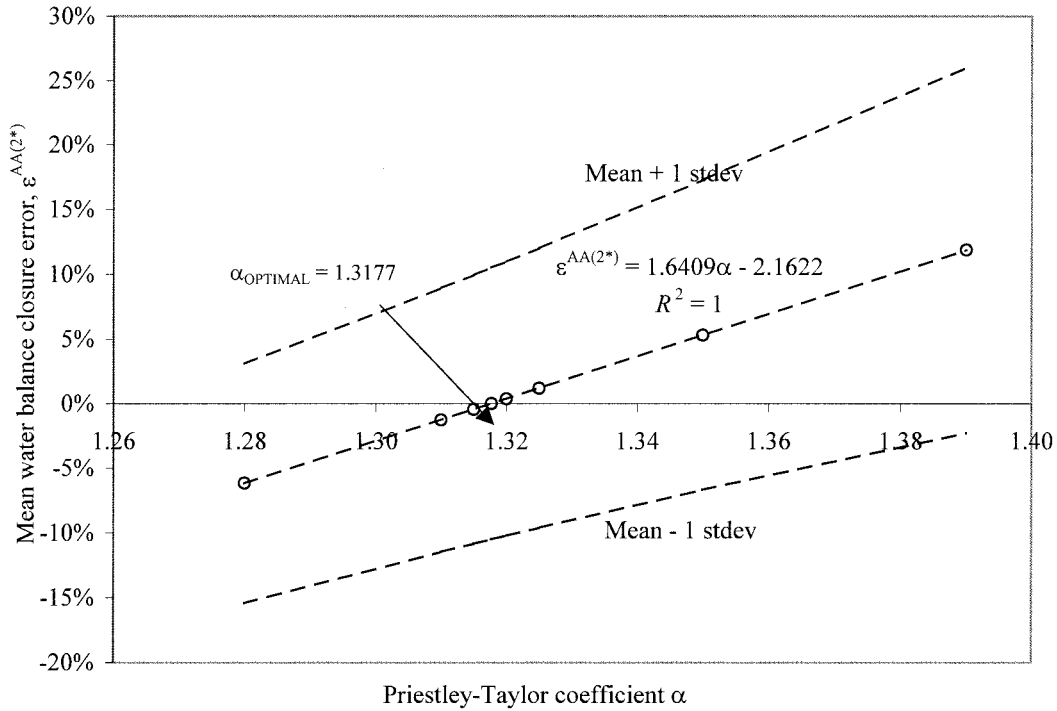


Figure 5. Mean closure errors  $\epsilon^{AA(2^*)}$  versus Priestley-Taylor coefficient trial values  $\alpha$ .

### 5. Summary and Conclusions

The objectives of this study were to examine the Advection-Aridity model of the hypothesis of a complementary relationship between actual and potential regional evapotranspiration with respect to its treatment of advection and to attempt to improve the model. Evaluation proceeded by comparing evapotranspiration estimates produced by the original AA model with independent estimates obtained from long-term, large-scale wa-

ter balances. Improvements to the model took the form of including a monthly, regionally reparameterized wind function in the  $ET_p$  formulation to remove wind speed dependence and recalibrating the Priestley-Taylor coefficient  $\alpha$  in the  $ET_w$  formulation to remove the bias toward underestimation of  $ET_a$ .

As shown in Table 1, the original AA model presented by *Brutsaert and Stricker* [1979] performed poorly, generating, for the complete set of 139 basins, an average annual closure

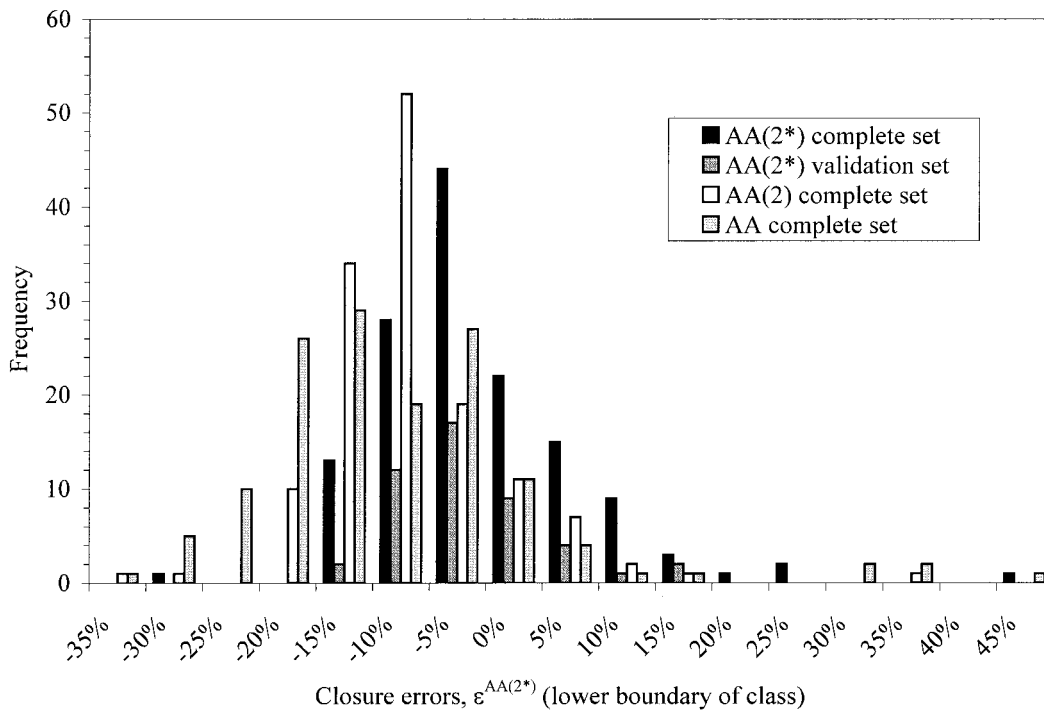


Figure 6a. Histogram of closure errors,  $\epsilon^{AA(2^*)}$ .

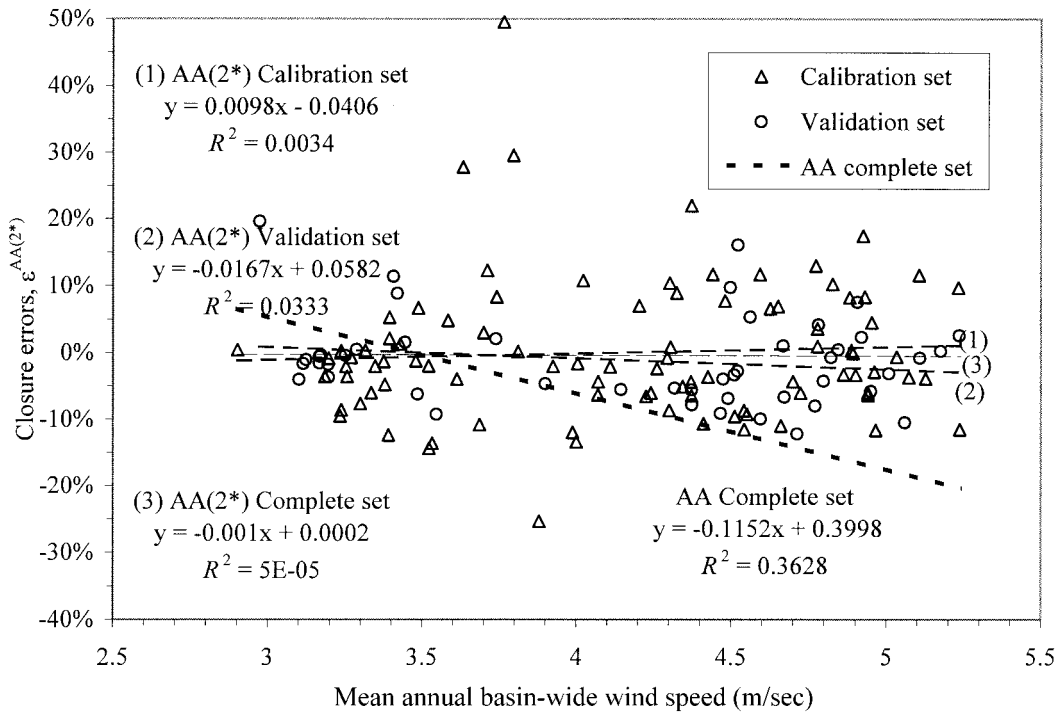


Figure 6b. Closure errors  $\epsilon^{AA(2^*)}$  versus mean annual basin-wide wind speed.

error of  $-7.92\%$  and a standard deviation of  $12.67\%$ . With the exception of a few outliers, which are discussed by *Hobbins et al.* [this issue], the general trend is toward negative AA closure errors. This may result from a poorly calibrated wind function.

The AA model's performance is affected by basin climatology. Except for the few outliers, closure error ( $\epsilon^{AA}$ ) becomes increasingly negative and variable with increasing aridity, indi-

cating that the predictive power of the AA model increases in moving toward regions of increased climate control of evapotranspiration rates and decreases in moving toward regions of increased soil control. Increased climate/soil control in this context refers to increased and decreased moisture availability, respectively. Because irrigated agriculture is often associated with areas of low moisture availability, these trends could be a reflection of anthropogenic influences, that is, through net

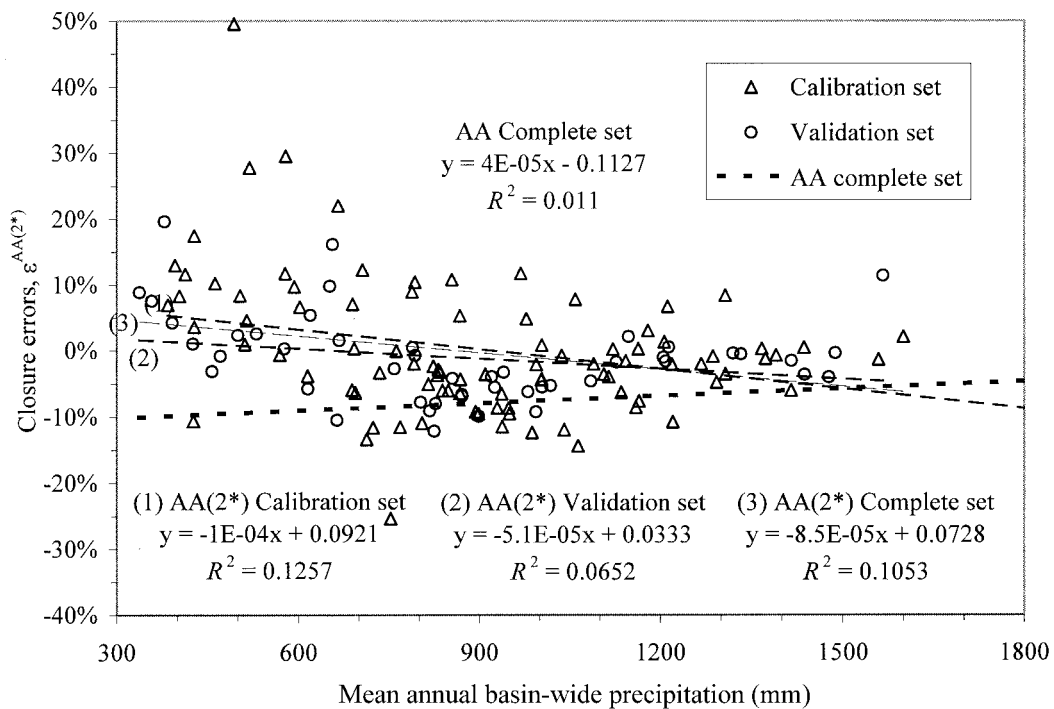
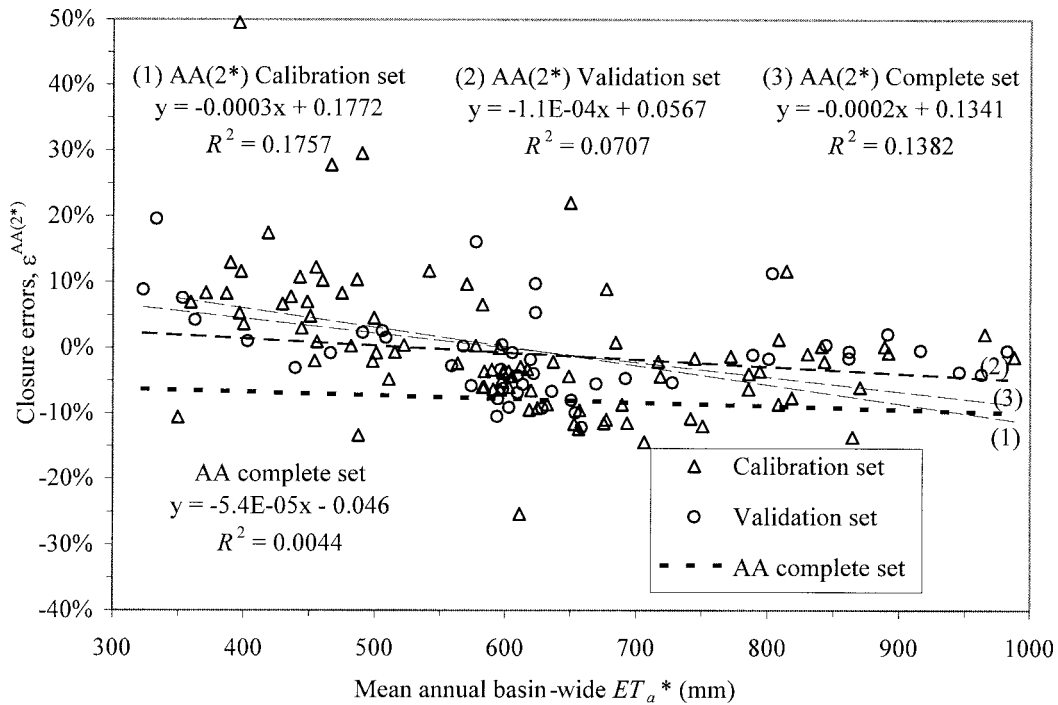


Figure 6c. Closure errors  $\epsilon^{AA(2^*)}$  versus mean annual basin-wide precipitation.



**Figure 6d.** Closure errors  $\varepsilon^{AA(2^*)}$  versus mean annual basin-wide  $ET_a^*$ .

groundwater withdrawals and net diversion of surface waters. However, as there were no groundwater usage data available, said anthropogenic effects were mitigated by selecting the basins, used for both recalibration and validation, from data sets of minimally impacted basins. However, it should be noted that groundwater pumping in a study basin affects only the independent evapotranspiration estimate  $ET_a^*$  not the  $ET_a^{MODEL}$  estimate. Indeed, one of the primary advantages of complementary relationship models is that their inherent assumption of the integration of atmospheric moisture accounts for all surface hydrology, and therefore their utility is unaffected in basins where groundwater pumping is present.

The AA model uses actual wind speed data to calculate the drying power of the air  $E_a$  in the expression for  $ET_p^{AA}$ . The strong positive correlation of the AA closure errors with wind speed clearly demonstrates the sensitivity of this model to the wind function  $f(U_2)$ , first proposed [Brutsaert and Stricker, 1979] for use in the AA model operating at a temporal scale of the order of days and highlights the need for a reparameterization of this component of  $ET_p^{AA}$  to yield both accurate  $ET_p$  estimates and unbiased water balance estimates on a monthly basis.

Although the use of  $ET_{pan}$  data to derive seasonal wind functions represents an independent means of reparameterizing the  $ET_p$  component of the AA model, as presented it does not produce any improvement in the model's treatment of advection. In fact, the modified model AA(1) performs significantly worse than the original AA model with the original Penman [1948] wind function. This is most likely due to experimental procedure. The stations recording the  $ET_{pan}$  may have been too far removed from the stations recording the aerological conditions. Many stations over much of the study area do not record  $ET_{pan}$  data outside of the growing season, leading to a paucity of data and a spatial bias in the  $ET_{pan}$  data used for these periods. The assumption that the data from the SAM-

SON stations accurately represent aerological conditions over homogenous areas large enough for the complementary relationship to hold is weak and easily violated.

The CRAE model, which calculates  $ET_p^{CRAE}$  by use of a vapor transfer coefficient  $f_T$  and does not use observations of wind speed, generates a near-zero mean annual closure error, thereby appearing to support the CRAE model's parameterization of the wind function. Using the  $ET_p^{CRAE}$  surfaces as proxy independent  $ET_p$  estimates and thereby replacing the original Penman wind function (5) with a regionally recalibrated, seasonal wind function yielded much improved results. The dependence of the closure errors on wind speed in the original AA model was removed in the AA(2) model, the mean closure error of the validation set of basins was reduced, in absolute terms, from  $-8.56\%$  to  $-7.93\%$ , and the standard deviation was reduced from  $13.45\%$  to  $5.32\%$ . Should a better data set, or even distributed  $ET_{pan}$  observations, become available at compatible temporal and spatial scales, this paper provides a methodology whereby they could be used in the seasonal, regional recalibration of the wind function.

Removal of the negative bias in the closure errors entailed optimizing the Priestley-Taylor coefficient  $\alpha$  subject to the constraint of a minimum mean closure error for a calibration subset of 92 basins. This procedure yielded a value of  $\alpha = 1.3177$ , very close to the value ( $\alpha = 1.32$ ) predicted by Morton [1983] in his reassessment of results reported by Priestley and Taylor [1972]. Use of  $\alpha = 1.3177$  with the regional, seasonal wind function further reduced, in absolute terms, the mean closure error of the validation set to  $-1.15\%$  and reduced the mean closure error of the complete set of 139 basins to  $-0.39\%$ . The standard deviation of the closure errors increased slightly to  $6.66\%$  for the validation set and to  $9.37\%$  for the complete set, which still represents a significant improvement over  $13.45\%$  for the validation set and  $12.67\%$  for the

complete set for the original *Brutsaert and Stricker* [1979] model.

The near-zero mean annual water balance closure errors for the CRAE model [see *Hobbins et al.*, this issue] and the improved seasonal, regional AA(2\*) model offered here indicate the utility of models based on the hypothesis of a complementary relationship in regional evapotranspiration for providing independent estimates of  $ET_a$ . For homogenous areas at regional scales these complementary relationship models are preferred over traditional evapotranspiration models using land-based parameterizations, as they implicitly account for the soil moisture dependence of potential evapotranspiration, their data requirements are significantly lighter, and they require no local calibration of parameters.

In summary, the regionally (i.e., USGS Water Resource Regions) and seasonally (i.e., monthly) enhanced  $ET_a$  model presented here (and referred to as the AA(2\*) model) has been parameterized to yield near-zero errors when run on a monthly scale and at a 10-km spatial scale within the spatial extent of the conterminous United States.

The values of the recalibrated parameters lie within reasonable physical bounds and are supported by those values already published in the literature. The parameter  $\alpha$  in the  $ET_w$  formulation is almost exactly as predicted by *Morton* [1983]. The reparameterization of the wind function yields values of  $f(U_2)$  that are comparable in scale to the predicted Penman values, although many region months exhibit counterintuitively negative  $f(U_2)$ - $U_2$  relationships.

This paper outlines procedures that enable reparameterization of the model for application in other regions. The wind function parameters derived for all season-region combinations are available from the authors and will appear in future work. Research continues into the behavior of these models in mountainous and high-elevation basins.

**Acknowledgments.** This work was partially supported by the US Forest Service and the National Institute for Global Environmental Change through the U.S. Department of Energy (Cooperative Agreement DE-FC03-90ER61010). In addition, one of the authors (Jorge A. Ramírez) received partial support from the Colorado Water Resources Research Institute. This paper benefited greatly from comments by Guido Salvucci and two other anonymous reviewers.

## References

- Allen, R. G., A Penman for all seasons, *J. Irrig. Drain. Eng.*, 112(4), 348–368, 1986.
- Bouchet, R. J., Evapotranspiration réelle evapotranspiration potentielle, signification climatique, *Symp. Publ. 62*, Int. Assoc. Sci. Hydrol., Berkeley, Calif., 134–142, 1963.
- Brutsaert, W., *Evaporation Into the Atmosphere: Theory, History, and Applications*, 299 pp., D. Riedel, Norwell, Mass., 1982.
- Brutsaert, W., and H. Stricker, An advection-aridity approach to estimate actual regional evapotranspiration, *Water Resour. Res.*, 15(2), 443–450, 1979.
- Davies, J. A., and C. D. Allen, Equilibrium, potential and actual evaporation from cropped surfaces in southern Ontario, *J. Appl. Meteorol.*, 12, 649–657, 1973.
- DeBruin, H. A. R., and J. Q. Keijman, Priestley-Taylor evaporation model applied to a large, shallow lake in the Netherlands, *J. Appl. Meteorol.*, 18(7), 898–903, 1979.
- Eagleson, P. S., Climate, soil and vegetation, 7, A derived distribution of annual water yield, *Water Resour. Res.*, 14(5), 765–776, 1978.
- Hobbins, M. T., J. A. Ramirez, T. C. Brown, and L. H. J. M. Claessens, Complementary relationship in the estimation of regional evapotranspiration: The Complementary Relationship Areal Evapotranspiration and advection-aridity models, *Water Resour. Res.*, this issue.
- McNaughton, K. G., and T. A. Black, Study of evapotranspiration from a Douglas-fir forest using energy-balance approach, *Water Resour. Res.*, 9(6), 1579–1590, 1973.
- Morton, F. I., Operational estimates of areal evapotranspiration and their significance to the science and practice of hydrology, *J. Hydrol.*, 66, 1–76, 1983.
- National Oceanic and Atmospheric Administration, *Solar and Meteorological Surface Observation Network 1961–1990* [CD-ROM], version 1.0, Natl. Clim. Data Cent., Asheville, N. C., 1993.
- Penman, H. L., Natural evaporation from open water, bare soil and grass, *Proc. R. Soc. London, Ser. A*, 193, 120–146, 1948.
- Priestley, C. H. B., and R. J. Taylor, On the assessment of surface heat flux and evaporation using large-scale parameters, *Mon. Weather Rev.*, 100, 81–92, 1972.
- Slack, J. R., and J. M. Landwehr, Hydro-climatic data network (HCDN): A U.S. Geological Survey streamflow data set for the United States for the study of climate variations, 1874–1988, *U.S. Geol. Surv. Open File Rep.*, 92-129, 1992.
- Stewart, R. B., and W. R. Rouse, A simple method for determining the evaporation from shallow lakes and ponds, *Water Resour. Res.*, 12(4), 623–628, 1976.
- Stewart, R. B., and W. R. Rouse, Substantiation of the Priestley and Taylor parameter  $\alpha = 1.26$  for potential evaporation in high latitudes, *J. Appl. Meteorol.*, 6, 649–650, 1977.
- U.S. Geological Survey, Class A pan evaporation for period 1931–1960, in *The National Atlas of the United States of America*, 417 pp., Washington, D. C., 1970.
- Van Bavel, C. H. M., Potential evaporation: The combination concept and its experimental verification, *Water Resour. Res.*, 2(3), 455–467, 1966.
- Wallis, J. R., D. P. Lettenmaier, and E. F. Wood, A daily hydroclimatic data set for the continental United States, *Water Resour. Res.*, 27(7), 1657–1663, 1991.
- Wright, J. L., New evapotranspiration crop coefficients, *J. Irrig. Drain. Div. Am. Soc. Civ. Eng.*, 108(IR2), 57–74, 1982.
- T. C. Brown, Rocky Mountain Research Station, U.S. Forest Service, Fort Collins, Colorado 80526-2098. (tcbrown@fs.fed.us)
- M. T. Hobbins and J. A. Ramirez, Department of Civil Engineering, Colorado State University, Fort Collins, CO 80523-1372. (mhobbins@lamar.colostate.edu; ramirez@engr.colostate.edu)

(Received December 20, 1999; revised November 2, 2000; accepted November 2, 2000.)

